



## ***Bifidobacterium pseudocatenulatum* ATCC 27919 exopolysaccharides induced autophagy and apoptosis against endoplasmic reticulum stress in Caco-2 cells**

Husna Zulkipli<sup>1</sup>, Hifa Nazirah Mohammed Yaziz<sup>2</sup>, Mohd Yusri Idorus<sup>3</sup>, Siti Hamimah Sheikh Abdul Kadir<sup>4</sup>, Maslinda Musa<sup>2</sup> and Khalilah Abdul Khalil<sup>2\*</sup>

<sup>1</sup>Faculty of Applied Sciences, Universiti Teknologi MARA, Perak Branch, 35400, Tapah Road, Perak, Malaysia.

<sup>2</sup>Department of Biomolecular Science, Faculty of Applied Sciences, Universiti Teknologi MARA, 40450 Shah Alam, Selangor, Malaysia.

<sup>3</sup>Institute of Medical Molecular Biotechnology (IMMB), Faculty of Medicine, Universiti Teknologi MARA, Sungai Buloh Campus, 47000 Sungai Buloh, Selangor, Malaysia.

<sup>4</sup>Faculty of Medicine, Universiti Teknologi MARA, Sungai Buloh Campus, 47000 Sungai Buloh, Selangor, Malaysia.  
Email: khali552@uitm.edu.my

Received 27 March 2023; Received in revised form 6 August 2023; Accepted 8 August 2023

### **ABSTRACT**

**Aims:** This study aimed to investigate the effect of exopolysaccharide (EPS) from *Bifidobacterium pseudocatenulatum* ATCC 27919 in Caco-2 cells on apoptotic and autophagic pathways.

**Methodology and results:** Cell viability was examined by MTS assay and it showed a significant decrease in Caco-2 cells after exposure to EPS. Microscopy imaging and morphological analyses demonstrated that EPS-exposed Caco-2 cells exhibited the main morphological characteristics of apoptosis. EPS-exposed cells showed early apoptosis and cell cycle arrest at the G2/M phase in the cell cycle and dead cell assays. qPCR suggested that mRNA expression of substantial apoptotic markers such as cleaved Caspase-3, BAX and PARP-1 were significantly increased in EPS-exposed cells. The autophagy event was demonstrated in EPS-exposed cells by the contrary mRNA expression of Beclin-1 and Bcl-2 and the detection of autophagic LC3-II protein at 24 h exposure. GRP78 mRNA expression was also increased in EPS-exposed cells, indicating the occurrence of endoplasmic reticulum (ER) stress.

**Conclusion, significance and impact of study:** Autophagy activity in EPS-exposed Caco-2 cells preceded apoptosis, suggesting it was a cytoprotective response against ER stress. Research findings set the foundation for therapeutic CRC treatments and provide insight into its regulatory processes.

**Keywords:** Apoptosis, autophagy, *Bifidobacterium pseudocatenulatum* ATCC 27919, colorectal cancer, exopolysaccharides

### **INTRODUCTION**

Based on the World Health Organization's (WHO) Globocan 2020 report, colorectal cancer (CRC) is the second most prevalent cancer among women after breast cancer (24.5%). It is men's third most common disease, accounting for 10.6% of all men's cancer cases (International Agency for Research on Cancer, 2020). It has been reported that the incidence of CRC is the second most frequent cancer among the general population in Malaysia (Ministry of Health Malaysia, 2021). Males in Malaysia are more likely to suffer colorectal cancer than females (16.9% vs. 10.7%), according to Azizah *et al.* (2019) in Malaysia National Cancer Registry (MNCR) 2012-2016 (Azizah *et al.*, 2019). The cancer is highly curable and manageable through early screening. In addition, according to the MNCR

2012-2016, around 70% of colorectal cancer patients in Malaysia were diagnosed with stage III or IV (Azizah *et al.*, 2019). The treatment is more difficult at this stage with worsening symptoms. The stage at diagnosis significantly impacts the course of treatment and the chance of survival. Furthermore, treatment's side effects and metastasis of chemo-resistant cells are the primary causes of low success rates and cancer recurrence. Additionally, CRC treatments can be costly and invasive for patients. Thus, it is necessary to investigate a new potential anti-cancer that aims to improve the effectiveness of the treatments. It includes studies on probiotics and the EPS from probiotics which have gained interest among researchers recently.

Probiotics are described as living bacteria that confer a health benefit to the host (FAO/WHO, 2006). Based on researchers' findings, probiotics positively affect the

\*Corresponding author

immune system and digestion (Anukam and Reid, 2007). Exopolysaccharides (EPS), including probiotic-derived ones, have been shown to contribute to the context (Oerlemans *et al.*, 2021). EPS is a functional biopolymer produced during the metabolic processes of bacteria. It is reported that EPS exhibits an extensive variety of physiological functions which includes immune regulation, antioxidant, anti-inflammation and anti-cancer (Angelin and Kavitha, 2020). Findings also revealed that EPS from probiotics improved symptoms of colon cancer through modulation of gut microbiota and metabolites, enhancing intestinal barrier function, suppressing NF- $\kappa$ B signalling pathway and lessening tumor burden (Zahran *et al.*, 2017; Lu *et al.*, 2019; Wu *et al.*, 2021). Hence, EPS has the potential to be applied as a complementary or alternative cancer treatment. *Lactobacillus* constitute a large group of potential probiotics and are found in diverse nutrition-rich habitats, including the food and gastrointestinal tract (GIT) of humans and animals (Duar *et al.*, 2017). They are prominent EPS producers and generally regarded as safe (GRAS). In recent years, *Lactobacillus*-derived EPS has extensively shown anti-proliferative effects on many types of tumor cells from the cervical, colon and liver (Sungur *et al.*, 2017; El-Deeb *et al.*, 2018; Jeong *et al.*, 2022). Parallely, *Bifidobacterium* presence in abundance with the *Lactobacillus* within human GIT also produced EPS. However, its physiological functions have not been widely explored in susceptibility to cancer treatments.

Current research focuses on developing anti-cancer treatments with lower or no side effects on the immune system than present synthetic medicines. Additionally, *Lactobacillus*-derived EPS has established pro-apoptotic attributes against a vast range of cancer cells (Wu *et al.*, 2021). It has been a goal in clinical oncology to eliminate cancer cells as they can evade apoptosis. The interaction of apoptosis with other signalling mechanisms, such as autophagy, has also emerged as potential cancer therapy (Qian *et al.*, 2017). Autophagy is an evolutionarily conserved catabolic process that maintains cellular homeostasis by breaking down unwanted or defective organelles and proteins. It has a controversial role in cancer, potentially contributing to the progression of the disease while also preventing tumor formation (Li *et al.*, 2020). Additionally, some signaling pathways, including AMP-activated protein kinase (AMPK) and mTOR (Dossou and Basu, 2019), are considered to be involved in regulating autophagy. Previous work shows an association between autophagy, apoptosis and related factors in colorectal cancer (Xie *et al.*, 2020).

Endoplasmic reticulum (ER) stress is a newly discovered apoptotic pathway along with death receptor and mitochondrial damage pathways (Xi *et al.*, 2022). It initially activates unfolded protein response (UPR) mechanism, which is known to induce autophagy (Bhardwaj *et al.*, 2020). It was evidenced that triggering excessive ER stress induces autophagy in cancer cells and eventually causes apoptotic cell death (Rah *et al.*, 2015). Here is a close connection between autophagy and apoptosis: Autophagy and apoptosis frequently interact, and both processes can either promote or hinder

the other. One of the primary causes of cancer may be the disruption of the dynamic balance between autophagy and apoptosis, which determine the fate of the cells.

Hence, the present study aims to determine the effects of EPS from *Bifidobacterium pseudocatenulatum* ATCC 27919 exposure in Caco-2 cells on cell death, including apoptosis and its interaction with autophagy with ER stress.

## MATERIALS AND METHODS

### Cell culture

The Caco-2 (ATCC<sup>®</sup> Cat. No. HTB-37<sup>™</sup>) cell line was purchased from the American Type of Cell Culture (ATCC). The cells were routinely cultured in Dulbecco's modified Eagle's minimal essential medium (DMEM; NECC, Sigma, Basel, Switzerland), which consists of vitamins, amino acids such as glutamine and 4500 mg/L glucose, supplemented with 10% (v/v) Foetal Bovine Serum (FBS; Gibco, Thermo Fisher Scientific, USA), 100 U/mL Penicillin and 100 mg/mL Streptomycin (Sigma, Switzerland). Phenol red (as pH indicator) and sodium bicarbonate were added to the media. A twenty-five cm<sup>2</sup> cell culture flask (T-25 flask) was used to culture the cells in an incubator with 5% CO<sub>2</sub> and 95% air at 37 °C. The cells were seeded at 5 × 10<sup>4</sup> cells/cm<sup>2</sup> density.

### Preparation of EPS from *Bifidobacterium pseudocatenulatum* ATCC 27919 and Rapamycin

The EPS was extracted from cultured probiotic *B. pseudocatenulatum* ATCC 27919 in cooked glutinous rice wastewater (RW) (Yaziz *et al.*, 2021). Analysis for monosaccharides composition was performed using acid hydrolysis, thin layer chromatography (TLC), high-performance liquid chromatography (HPLC-RID) and Fourier-transformed infrared spectroscopy (FT-IR) (Yaziz *et al.*, 2021). Exopolysaccharides (EPS) were weighed and dissolved in Dulbecco's modified Eagle's minimal essential medium (DMEM; NECC, Sigma, Basel, Switzerland) culture media for 10 mL of working solution.

About 1 mM stock solution of Rapamycin (Gold Biotechnology, St. Louis, MO) was prepared by dissolving 5 mg of Rapamycin in 5 mL DMSO. Next, the stock solution was dissolved in DMEM culture medium accordingly to desired working solutions which were 10  $\mu$ M, 20  $\mu$ M, 30  $\mu$ M, 40  $\mu$ M and 50  $\mu$ M. The stock solution was kept at -20 °C until further use. The working solutions were prepared instantly before the experiments.

### Cell viability assay by MTS

Caco-2 cells were cultured in a 96-well plate at a seeding density of 10<sup>4</sup> cells/cm<sup>2</sup> at 37 °C in a humidified, 5% CO<sub>2</sub> atmosphere. After reaching 80% cell confluent, the cells were washed with PBS buffer and the culture medium was replaced with Rapamycin and EPS at working solution concentrations: 1 mg/mL, 5 mg/mL and 10 mg/mL. Following 24 and 48 h of incubation, 20  $\mu$ L of

CellTiter 96® AQueous One Solution Reagent contains a novel tetrazolium compound [3-(4,5-dimethylthiazol-2-yl)-5-(3-carboxymethoxyphenyl)-2-(4-sulfophenyl)-2H tetrazolium (MTS)] was pipetted into each well of the 96-well assay plate containing the treated cells in 100 µL of culture medium. The 96-well plate was incubated at 37 °C for 2 h in a humidified, 5% CO<sub>2</sub> atmosphere. According to the manufacturer's protocol, absorption was measured at 490 nm using Victor™ X Series Multilabel Plate Reader (PerkinElmer, Boston).

### Cell cycle analysis

Caco-2 cells were cultured in T-25 flasks at a seeding density of  $5 \times 10^4$  cells/cm<sup>2</sup>. After indicated treatments, detached cells were collected. The pellets from trypsinization were suspended in PBS and transferred into a centrifuge tube for fixation in ethanol. Approximately 1 mL of ice-cold ethanol 70% ethanol was added to the suspension while vortexing at medium speed to get a uniform ethanol-fixed cell suspension. Fixed cells were frozen at -20 °C for 3 h before staining. Ethanol-fixed cells were centrifuged two times for 5 min at room temperature. The cell pellets were resuspended in PBS. The tubes were centrifuged again for 5 min and the supernatant was removed. The cell pellets were resuspended in 200 µL of Muse™ Cell Cycle Reagent and incubated for 30 min at room temperature, protected from light. The cell suspensions were transferred to a 1.5 mL microcentrifuge tube before analysis on Muse™ Cell Cycle Analyzer. The percentage of cells in the G0/G1, S, and G2/M phases was measured according to the manufacturer's instructions.

### Annexin V and cell dead analysis

Caco-2 cells were cultured in T-25 flasks at a seeding density of  $5 \times 10^4$  cells/cm<sup>2</sup>. After indicated treatments, detached cells were collected. The pellets from trypsinization were suspended in FBS. 100 µL of each cell suspension was transferred to a 1.5 mL microcentrifuge tube and 100 µL of the Muse™ Annexin V and Dead Cell Reagent to each tube. The tubes were gently vortexed and incubated for 20 min at room temperature in the dark before analysis on Muse™ Cell Cycle Analyzer. Four populations of cells were distinguished by four quadrants in this assay according to the manufacturer's instructions.

### DAPI immunofluorescence staining

Caco-2 cells were cultured in chamber slides at a seeding density  $5 \times 10^4$  cells/cm<sup>2</sup>. After indicated treatments, growth media with EPS and Rapamycin were removed from the cells. Cells were washed once with PBS. The cells were fixed with 4% paraformaldehyde for 24 h. Next, cells were rehydrated with 1× PBS for 10 min. Cells on the slide were blocked with 2% BSA in 1× PBS at room temperature for 60 min. It was followed by staining with 300 nM DAPI staining solution. 300 µL of diluted DAPI staining solution was added. Cells were incubated for 5

min in the dark at room temperature. Next, cells were rinsed several times with PBS. Excess PBS was drained. A mounting medium, Prolong® Gold antifade reagent, was added to the slides to protect the stain from fading (photobleaching). Coverslip was slowly put in to avoid trapping any air bubbles. Image viewing was performed using Leica TCS SP5 confocal microscope at 10× and 40× magnification.

### Autophagy detection by LC3 expression assay

Caco-2 cells were cultured in a 96-well plate at a seeding density  $1 \times 10^4$  cells/cm<sup>2</sup>. After indicated treatments, cells were washed with Hanks' Balanced Salt Solution (HBSS) (Merck, Darmstadt, Germany). Media was replaced with Earle's Balanced Salt Solution (EBSS) (Merck, Darmstadt, Germany) and autophagy Reagent A (1:1000 dilution to induce autophagy under starvation conditions. After 4 h treatment, the cells were detached with Accutase, Invitrogen™ (Thermo Fischer Scientific, USA). One (1)× HBSS was added to the cells before transferring them into Muse-compatible sample tubes. The sample tubes were spun and the supernatants were removed. For staining, 5 µL Anti-LC3 Alexa Fluor®555 and 95 µL of 1× Autophagy Reagent B were added to each sample. Samples were stained on ice for 30 min in the dark. The sample tubes were spun and supernatants were removed. The cells were washed with 1× Assay Buffer, and each sample was resuspended in 200 µL 1× Assay Buffer. The samples were acquired on Muse™ Cell Cycle Analyzer immediately. During acquisition, event counts per µL were assured below 800. The acquisition was performed according to manufacturer instructions.

### mRNA extraction and quantitative PCR (qPCR)

Total RNA for qPCR was extracted from cells using innuPREP RNA Mini Kit 2.0 (Analytik Jena, GmbH, Germany). RNA quality extracted was analyzed using a Bioanalyzer system (Agilent, Santa Clara, CA, USA). Total RNA (50 ng/µL) was reverse transcribed using SensiFAST™ cDNA Synthesis Kit (Bioline USA Inc., USA). qPCR was performed using SensiFAST™ SYBR® No-ROX Kit (Bioline USA Inc., USA). The program for qPCR was set up in Bio-Rad CFX96 Touch Real-Time PCR Detection System thermal cycler under the following conditions: 2 min at 95 °C followed by 30 cycles of 95 °C for 5 sec, 60-65 °C for 10 sec and 72 °C for 5-20 sec. GAPDH and HPRT1 genes were used as reference genes to normalize the expression of genes of interest. The primers used are as in Table 1.

### Protein expression via phosphorylation enzyme-linked immunosorbent assay (ELISA)

Caco-2 cells were cultured in T-25 flasks at a seeding density of  $5 \times 10^4$  cells/cm<sup>2</sup>. After indicated treatments, the cells were detached using Trypsin-EDTA. Cells were standardized at  $4 \times 10^6$  cells/mL. All the medium flasks were then transferred into 15 mL centrifuge tubes.

**Table 1:** Primer sequences.

Gene	Primer sequence
GAPDH	F: ACC GCG AGA AGA TGA CCC AG R: GGA TAG CAC AGC CTG GAT AGC AA
HPRT1	F: CAT TAT GCT GAG GAT TTG GAA AGG R: CTT GAG CAC ACA GAG GGC TAC A
BECLIN-1	F: AAG ACG TCC AAC AAC AGC AC R: CTT CCT CCT GGG TCT CTC CT
BCL-2	F: ATC GCC CTG TGG ATG ACT GAG T R: GCC AGG AGA AAT CAA ACA GAG GC
PARP1	F: CGC ATA CTC CAT CCT CAG TG R: GGA TCA GGG TGT AAA AGC GAT
BAX	F: TCA GGA TGC GTC CAC CAG AAG R: TGT GTC CAC GGC GGC AAT CAT C
GRP78	F: ACA TCA AGT TCT TGC CGT TCA A R: ATA AGC CTC AGC GGT TTC TTT C

F, forward; R, reverse.

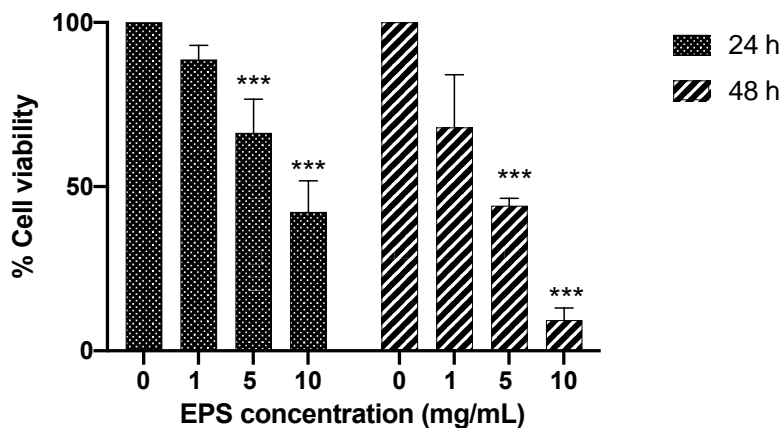


**Figure 1:** Effect of different concentrations of EPS from *B. pseudocatenulatum* ATCC 27919 exposure on Caco-2 cells viability after 24 and 48 h. At 5 and 10 mg/mL EPS and after 24- and 48 h exposure, significant cell viability reduction was observed compared to unexposed Caco-2 cells (control). Data were expressed as mean  $\pm$  SD. \*\*\* $p$ <0.001 compared to the negative control (unexposed),  $n=3$ .

All the cell suspension was collected and centrifuged for 5 min. The supernatant was discarded, the cell pellet was rinsed with PBS buffer before cell lysate preparation and assay procedures were performed according to the manufacturer's instructions. The protein markers tested were Phospho-mTOR, Phospho-AMPK- $\alpha$ 1, Cleaved-Caspase-3, p53 and p62.

#### Statistical analysis

Statistical analysis was performed using GraphPad Prism version 8.0.1 (GraphPad Software, California, USA). The data were presented as mean  $\pm$  SD for replicates generated from at least three experiments ( $n=3$ ). The data were checked for normality tests and analyzed using two-way ANOVA. It is followed by post hoc test recommended, Tukey's. The results were statistically significant at  $p$ <0.05,  $p$ <0.01 and  $p$ <0.001.

#### RESULTS

##### EPS from *Bifidobacterium pseudocatenulatum* ATCC 27919 and Rapamycin effectively suppressed cell viability in Caco-2 cells

To determine the effect of EPS from *B. pseudocatenulatum* ATCC 27919, cell viability was measured in Caco-2 cells exposed at different concentrations of EPS (1, 5 and 10 mg/mL) and time-point (24 and 48 h) by MTS assay. In 5 mg/mL EPS-exposed Caco-2 cells, it was observed that cell viability was significantly ( $p$ <0.001) reduced after 24 h (66.6%) and 48 h (46.2%) exposure when compared to unexposed cells. A similar but more potent and significant ( $p$ <0.001) reduction was observed in 10 mg/mL EPS-exposed Caco-2 cells after 24 (42.3%) and 48 h (9.4%). However, their cell viability was not significantly observed with 1 mg/mL of EPS exposure (Figure 1).

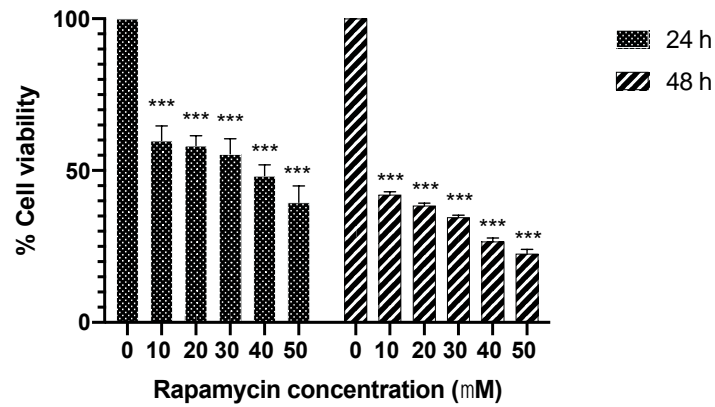


**Figure 2:** Effect of different concentrations of Rapamycin exposure on Caco-2 cell viability after 24 and 48 h. All tested concentrations of Rapamycin showed a significant reduction in cell viability against unexposed cells with a more potent effect after 48 h of exposure. Data were expressed as mean  $\pm$  SD. \*\*\* $p < 0.001$  compared to negative control (unexposed cells),  $n = 3$ .

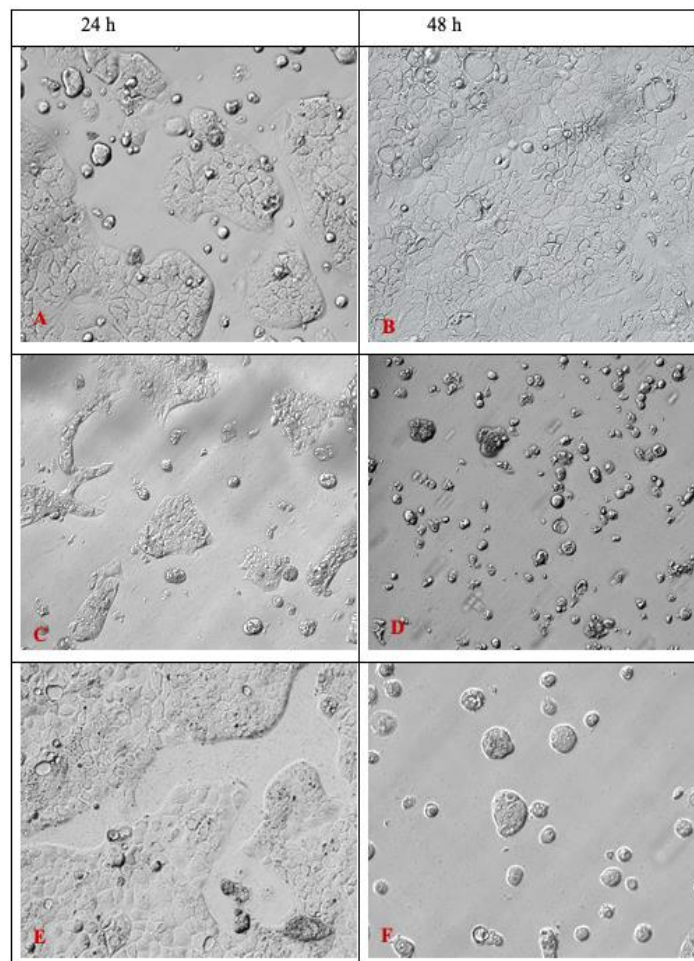


**Figure 3:** Microscopy images of Caco-2 cells after exposure at 24 h and 48 h (10 $\times$  and 40 $\times$  magnification). (A-B) unexposed Caco-2 cells at 24 and 48 h, (C-D) Caco-2 cells exposed to Rapamycin at 24 and 48 h, (E-F) Caco-2 cells exposed to EPS from *Bifidobacterium pseudocatenulatum* ATCC 27919 at 24 and 48 h. Exposure to Rapamycin and EPS caused shrinkage of Caco-2 cells with apoptotic features and detached from the culture plate.

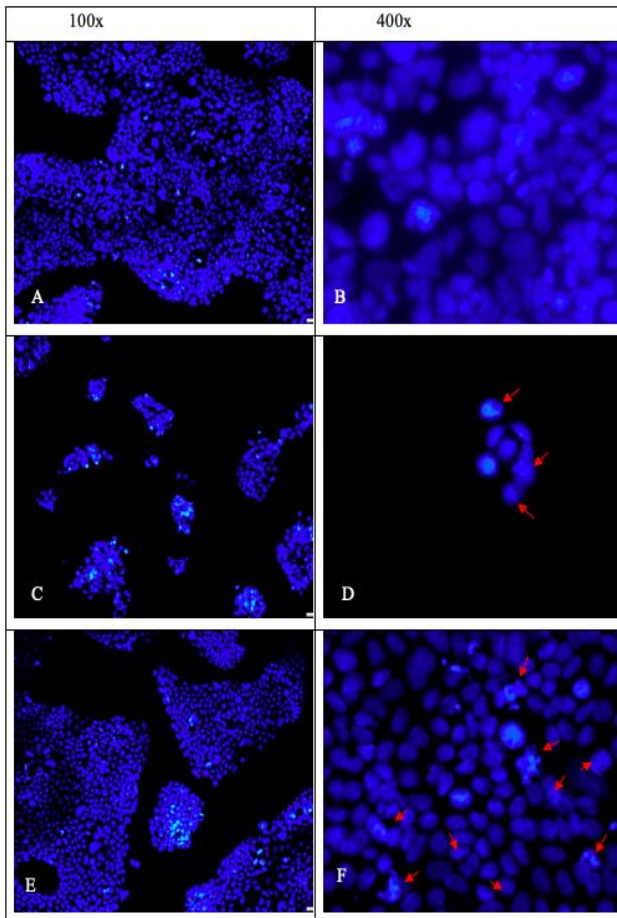


**Figure 4:** DAPI nuclear staining of Caco-2 cells DAPI exposed to EPS from *B. pseudocatenulatum* ATCC 27919 and Rapamycin after 24 h (10x and 40x magnification). (A-B) unexposed cells, (C-D) cells exposed to Rapamycin and (E-F) cells exposed to EPS. Red arrows indicate shrunk cells with condensed nuclei and loss of shape.

Cell viability was also measured in Caco-2 cells exposed to Rapamycin at various concentrations (10, 20, 30, 40 and 50  $\mu\text{M}$ ) and time-point (24 and 48 h) (Figure 2). All the concentrations exposed to Caco-2 cells reduced cell viability significantly when compared to unexposed cells after 24 h (10  $\mu\text{M}$  = 59.8%, 20  $\mu\text{M}$  = 58.2%, 30  $\mu\text{M}$  = 55.5%, 40  $\mu\text{M}$  = 48.3% and 50  $\mu\text{M}$  = 39.5%). However, a more potent effect was observed after 48 h (10  $\mu\text{M}$  = 42%, 20  $\mu\text{M}$  = 38.4, 30  $\mu\text{M}$  = 34.6%, 40  $\mu\text{M}$  = 26.6% and 50  $\mu\text{M}$  = 22.6%). In this study, Rapamycin was used to induce autophagy in the Caco-2 cells (Jangamreddy *et al.*, 2015) and it was designated as a positive control group for the experiments.

Subsequent experiments were performed using a concentration of 5 mg/mL of EPS and 30  $\mu\text{M}$  of Rapamycin (as positive control). 10 mg/mL of EPS was not used as the culture medium became turbid when prepared.

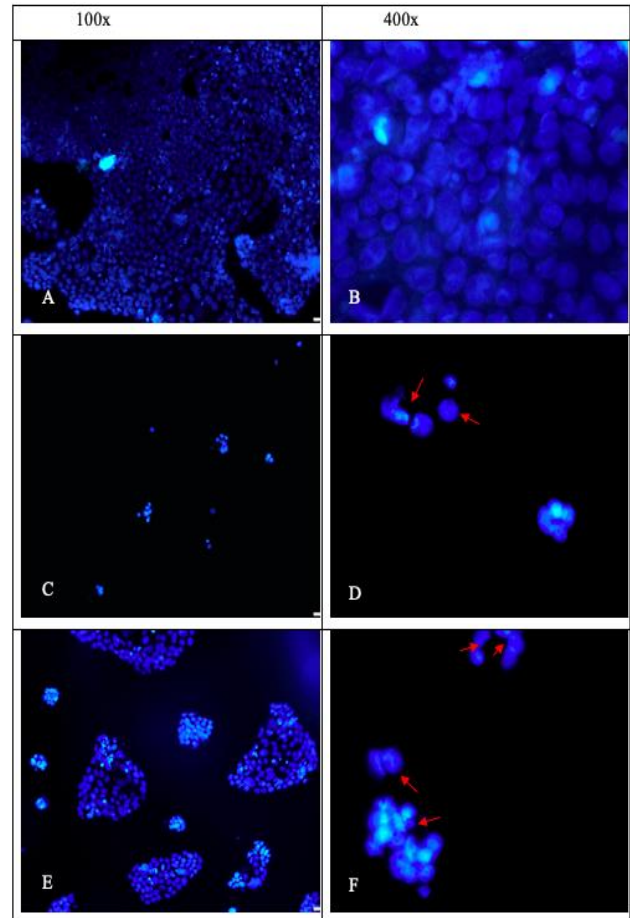


**Figure 5:** DAPI nuclear staining of Caco-2 cells DAPI exposed to EPS from *B. pseudocatenulatum* ATCC 27919 and Rapamycin after 48 h (10x and 40x magnification). (A-B) unexposed cells, (C-D) cells exposed to Rapamycin and (E--F) cells exposed to EPS. Red arrows indicate shrunk cells with condensed nuclei and loss of shape.

#### Apoptosis contributes to EPS-induced cell death in Caco-2 cells

An inverted light microscope visually observed Caco-2 cells to investigate the effect of EPS exposure for 24 and 48 h. In EPS-exposed cells (Figure 3C and D), more dead and detached cells from the flask surface were observed than unexposed cells. Likewise, a similar observation was observed in Rapamycin-exposed cells (Figures 3E and F). Cell shrinkage, one of the apoptotic features, was observed distinctly in both EPS and Rapamycin-exposed cells after 24 h and 48 h.

The EPS-exposed cells also exhibited smaller sizes due to cell shrinkage and condensed nuclei and they lost shape. As previously mentioned in the microscopy visualization section, EPS-exposed cells have undergone cell death and detached from the culture plate surface, decreasing the number of blue-stained cells (Figure 4F

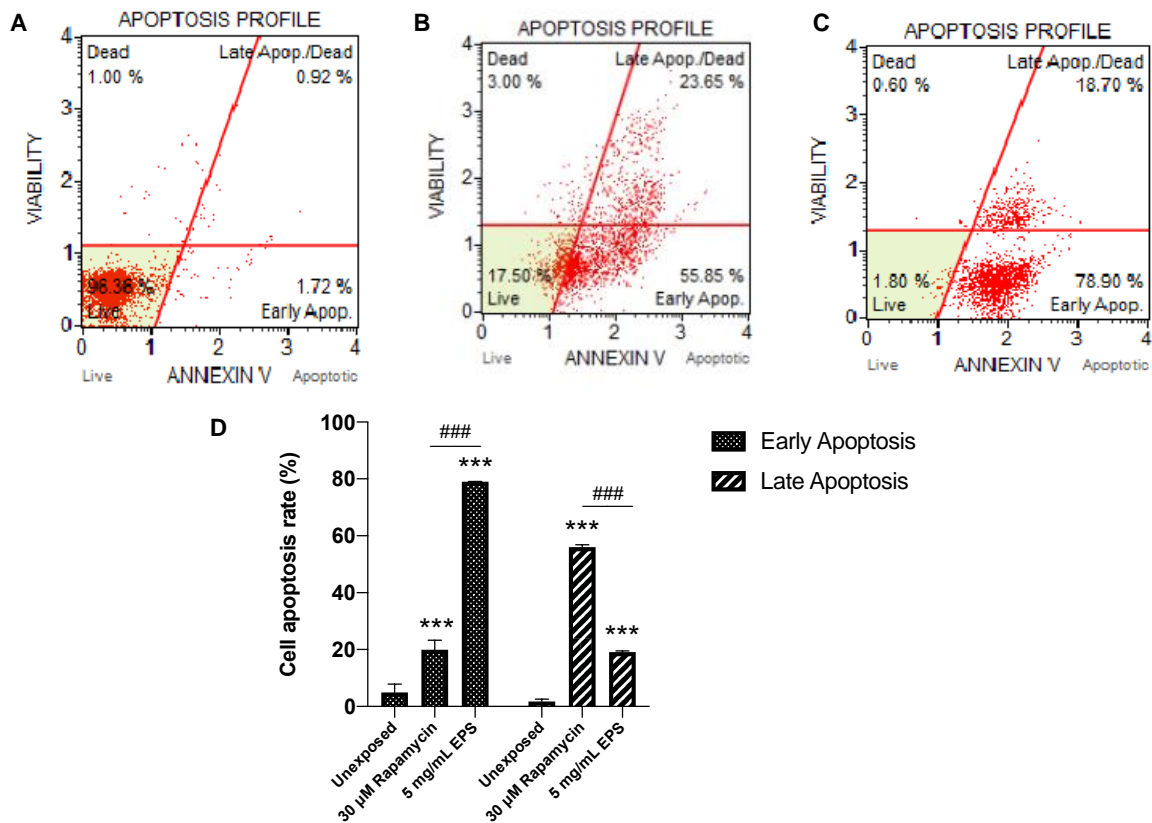


**Figure 6:** Annexin V and dead cell assay of Caco-2 cells exposed to EPS from *B. pseudocatenulatum* ATCC 27919 and Rapamycin for 48 h. (A) unexposed cells, (B) cells exposed to Rapamycin and (C) exposed to EPS from *B. pseudocatenulatum* ATCC 27919. (D) Chart comparison of cell distribution after the exposure of EPS and Rapamycin for 48 h. Data were expressed as mean  $\pm$  SD. \*\*\* $p < 0.001$  compared to negative control (unexposed cells), ### $p < 0.001$  compared to positive control (Rapamycin),  $n = 3$ .

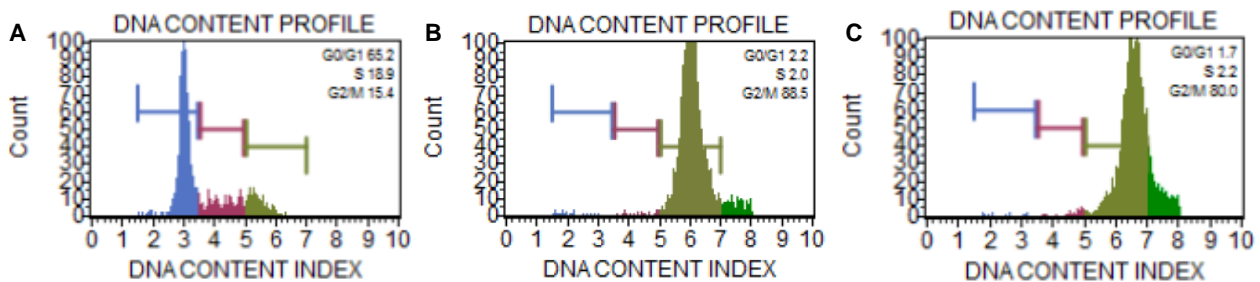


**Figure 7:** Cell cycle arrest of Caco-2 cells exposed to EPS from *B. pseudocatenulatum* ATCC 27919 and Rapamycin for 48 h and analysed by flow cytometry. (A) Cell cycle was arrested at G0/G1 phase in unexposed cells, (B) cell cycle was arrested at the G2/M phase when exposed to Rapamycin and (C) cell cycle was arrested at the G2/M phase when exposed to EPS from *B. pseudocatenulatum* ATCC 27919.

and Figure 5F). Additionally, Rapamycin-exposed cells exhibited comparable observations as EPS-exposed but with a more prominent effect (Figure 4D and Figure 5D). However, the unexposed cells mostly remained intact and uniformly in the shape after 24 and 48 h.

Annexin V and dead cell assay were also used to verify the findings to detect apoptotic cells. There was

minimal cell distribution in Q1, Q2 and Q4 in unexposed cells, indicating a very low amount of necrotic, early and late apoptotic cells, respectively. Most viable cells can be seen in Q3 (Figure 6A). The cell distribution shifted more to Q2 (23.65%) and Q4 (55.85%) after the exposure of 30 µM Rapamycin leaving 17.50% of viable cells in Q3. Only 3.0% of cells were observed in Q1 (Figure 6B). In EPS-

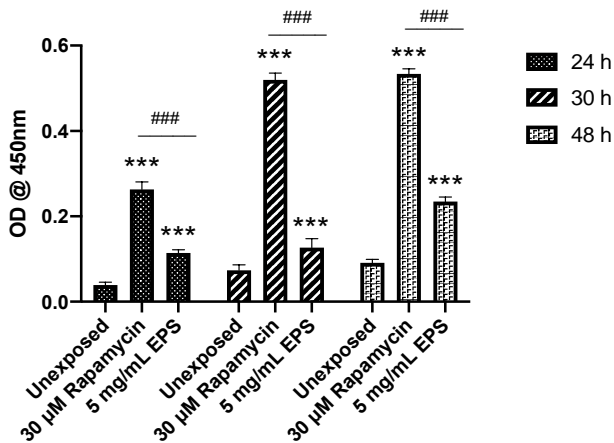


**Figure 8:** Cleaved Caspase-3 protein expression was elevated in EPS from *B. pseudocatenulatum* ATCC 27919-exposed cells and Rapamycin-exposed cells compared to unexposed cells throughout all time. Data were expressed as mean  $\pm$  SD. \*\*\* $p$ <0.001 compared to control (unexposed cells), ### $p$ <0.001 compared to positive control (Rapamycin),  $n=3$ .

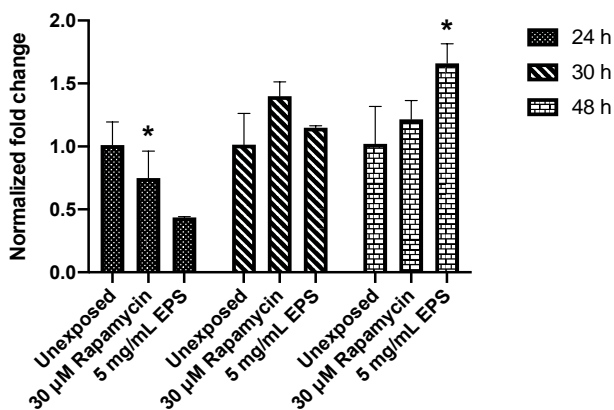


**Figure 9:** mRNA expression of BAX was upregulated in EPS from *B. pseudocatenulatum* ATCC 27919-exposed cells and Rapamycin-exposed cells at 30 and 48-h time points compared to unexposed cells. Data were expressed as mean  $\pm$  SD. \* $p$ <0.05 compared to negative control (unexposed cells),  $n=3$ .

exposed cells, the cell distribution exhibited a percentage of 78.90% in Q4 representing early apoptosis. While for Q2, late apoptosis, there are 18.70% cells in the quadrant. 1.8% and 0.6% cells were in Q3 and Q1 respectively (Figure 6C). Summarily, EPS has caused a significant increase in apoptosis in Caco-2 cells, as seen by the overall cell population shift (Figure 6D).

Analysis of the cell cycle revealed the phases in which the cell cycle was arrested following the exposure of Caco-2 cells to EPS and 30  $\mu$ M Rapamycin for 48 h. In unexposed cells (Figure 7A), 65.2% of the cell population

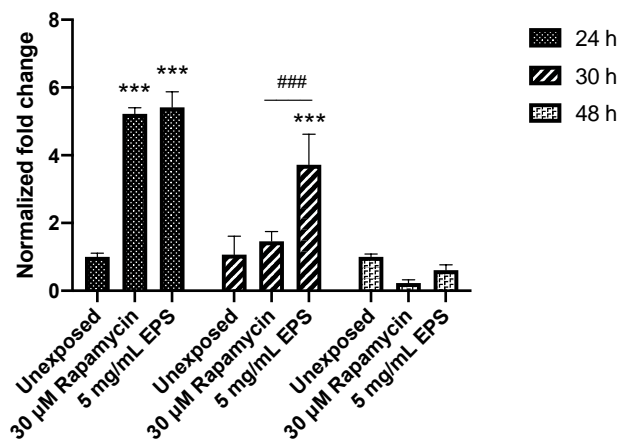


**Figure 10:** mRNA expression of PARP1 was significantly upregulated in EPS from *B. pseudocatenulatum* ATCC 27919-exposed cells and Rapamycin-exposed cells at 24 h of exposure compared to unexposed cells. Data were expressed as mean  $\pm$  SD. \*\*\* $p$ <0.001 compared to negative control (unexposed cells), ### $p$ <0.001 compared to positive control (Rapamycin),  $n=3$ .

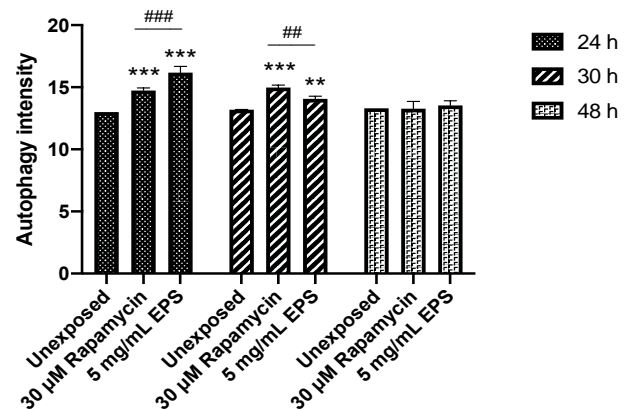


**Figure 11:** EPS from *B. pseudocatenulatum* ATCC 27919-exposed cells and Rapamycin-exposed cells showed significant autophagy intensity compared to the unexposed cells based on the quantification of LC3-II, specifically after 24 h of exposure. Data were expressed as mean  $\pm$  SD, \*\* $p$ <0.01, \*\*\* $p$ <0.001 compared to negative control (unexposed cells), ### $p$ <0.001, ## $p$ <0.01 compared to positive control (Rapamycin),  $n=3$ .

was arrested in the G0/G1 phase, while 18.9% and 15.4% were arrested at S and G2/M phases. However, the cell population was notably arrested during the G2/M phase when exposed to Rapamycin and EPS for 48 h with a percentage of 88.5% and 80%, respectively, compared to unexposed cells. (Figure 7B and 7C).

In addition, it was observed that EPS exposure significantly ( $p$ <0.001) enhanced the protein expression of cleaved Caspase-3 in Caco-2 cells compared to

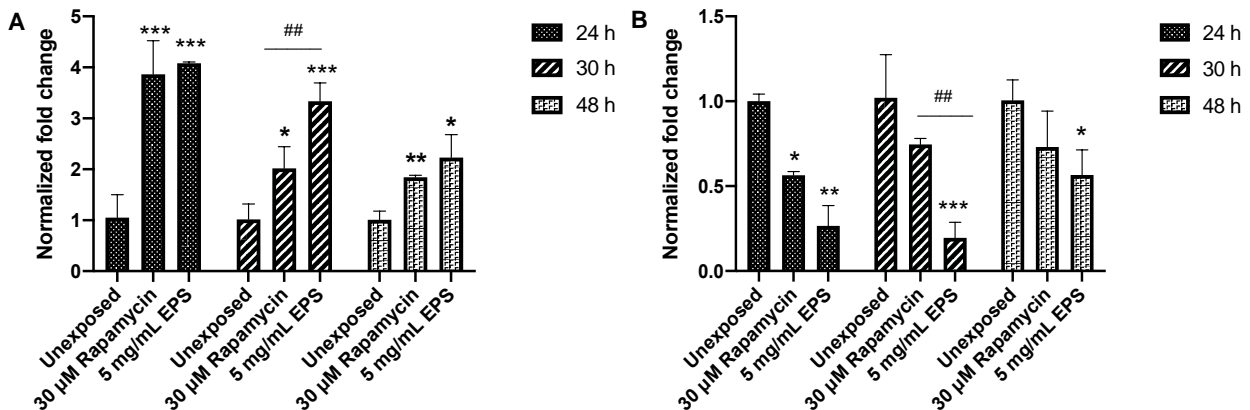


**Figure 12:** (A) mRNA expression of Beclin-1 was significantly upregulated in EPS from *B. pseudocatenulatum* ATCC 27919-exposed cells and Rapamycin-exposed cells at 24 h but reduced in an extended time compared to unexposed cells. (B) mRNA expression of Bcl-2 in EPS from *B. pseudocatenulatum* ATCC 27919-exposed cells and Rapamycin-exposed cells was significantly reduced compared to unexposed cells throughout all the time-point. Data were expressed as mean  $\pm$  SD. \* $p < 0.05$ , \*\* $p < 0.01$ , \*\*\* $p < 0.001$  compared to negative control (unexposed cells), ## $p < 0.01$  compared to positive control (Rapamycin),  $n = 3$ .

unexposed cells. Parallely, Rapamycin exposure showed a similar significant trend of protein expression but with a greater effect (Figure 8). We also found that EPS upregulated the mRNA expression of BAX, especially at the 48-h time point ( $1.66 \pm 0.15$ -fold) ( $p < 0.01$ ) but not at the 24-h time point. The observation is also comparative to Rapamycin-exposed cells (Figure 9). PARP-1 mRNA expression was upregulated with  $5.41 \pm 0.46$ -fold change at 24 h and  $3.72 \pm 0.9$ -fold change at 30 h time point but downregulated upon exposure to EPS and Rapamycin at 48 h (Figure 10).

#### Autophagy preceded the apoptosis cell death in EPS-exposed Caco-2 cells

Autophagy is likely the possible underlying mechanism of apoptosis activation in cancer therapy (Bata and Cosford, 2021). We investigated if EPS exposure could induce autophagy in Caco-2 cells to verify the mechanism by measuring autophagic protein LC3-II. As shown in Figure 11, EPS exposure significantly increased autophagy intensity compared to the unexposed cells after 24 h ( $p < 0.001$ ). However, the autophagy intensity started to reduce after 30-h exposure. At 48-h exposure, no significant increase in autophagy was observed compared to unexposed and Rapamycin-exposed cells.

To evaluate EPS-induced autophagy dependency on Beclin-1 (an essential autophagy component), mRNA expression of Beclin-1 and Bcl-2 were examined in Caco-2 cell exposed EPS and Rapamycin. Bcl-2 notably regulates the autophagy pathway by interacting with Beclin-1 to induce autophagy (Bata and Cosford, 2021). The mRNA expression of Beclin-1 was significantly upregulated  $4.08 \pm 0.028$ -fold at the 24-h time point compared to unexposed cells ( $p < 0.001$ ). In Rapamycin-exposed cells, the expression was significantly upregulated at  $3.87 \pm 0.68$ -fold compared to the

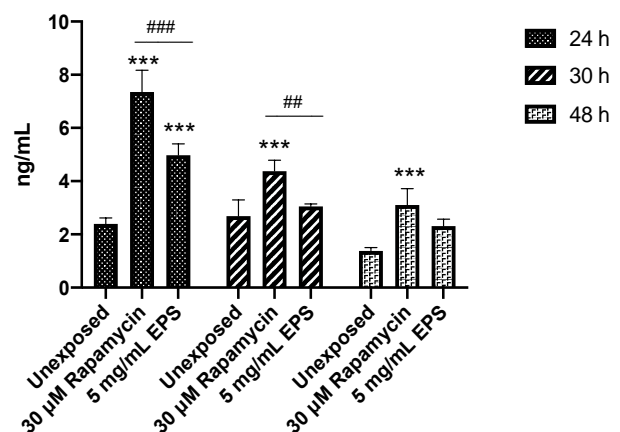


**Figure 13:** Protein expression of p62/SQSTM1 increased in EPS from *B. pseudocatenulatum* ATCC 27919-exposed cells and Rapamycin-exposed cells compared to unexposed cells. However, the expression was reduced as the time point tested extended to 30 and 48 h. Data were expressed as mean  $\pm$  SD. \*\*\* $p < 0.001$  compared to negative control (unexposed cells), ## $p < 0.01$ , ### $p < 0.001$  compared to positive control (Rapamycin),  $n = 3$ .

unexposed cells ( $p < 0.001$ ). (Figure 12A). On the other hand, Bcl-2 expression was downregulated in EPS and Rapamycin-exposed cells at all time points (Figure 12B).

To further confirm the induction of autophagy by EPS in the cells, protein expression of p62 or SQSTM1 was also examined. As demonstrated in Figure 13, the protein expression of p62 was significantly increased in EPS-exposed cells, especially at 24 h ( $p < 0.001$ ). Rapamycin-exposed cells showed higher protein expression of p62 simultaneously ( $p < 0.001$ ). On the other hand, a similar trend was observed with exposure to EPS and

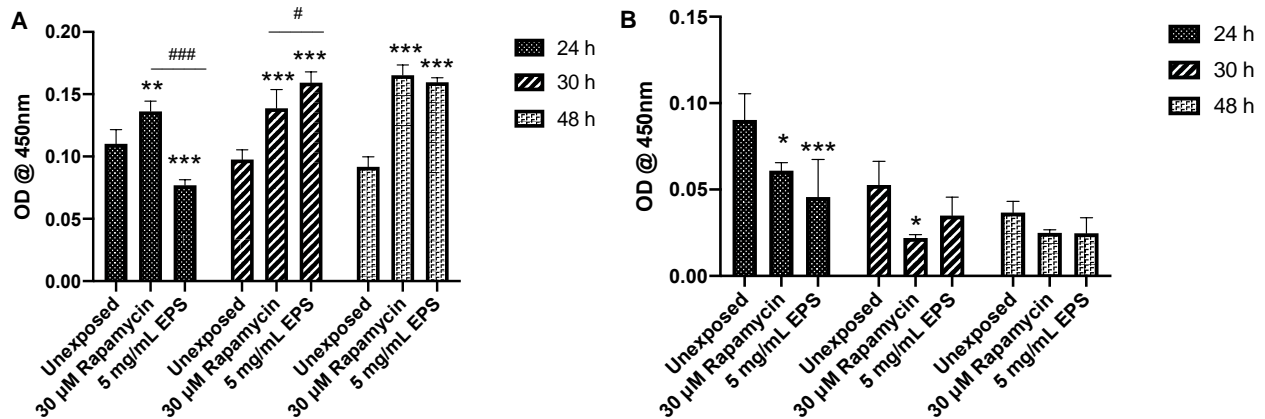


**Figure 14:** (A) Phosphorylated AMPK protein expression in EPS from *B. pseudocatenulatum* ATCC 27919-exposed cells was lower than unexposed and Rapamycin-exposed cells at 24 h. The protein expression increased at 30 and 48 h in EPS- and Rapamycin-exposed cells. Data was expressed as mean  $\pm$  SD. \*\* $p$ <0.01, \*\*\* $p$ <0.001 compared to negative control (unexposed cells), # $p$ <0.05, ###  $p$ <0.001 compared to positive control (Rapamycin),  $n$ =3. (B) Phosphorylated mTOR protein expression in EPS from *B. pseudocatenulatum* ATCC 27919-exposed cells was significantly reduced compared to unexposed cells throughout the observed time. The expression in Rapamycin-exposed cells was also similar. Data were expressed as mean  $\pm$  SD. \* $p$ <0.05, \*\*\* $p$ <0.001 compared to negative control (unexposed cells),  $n$ =3.

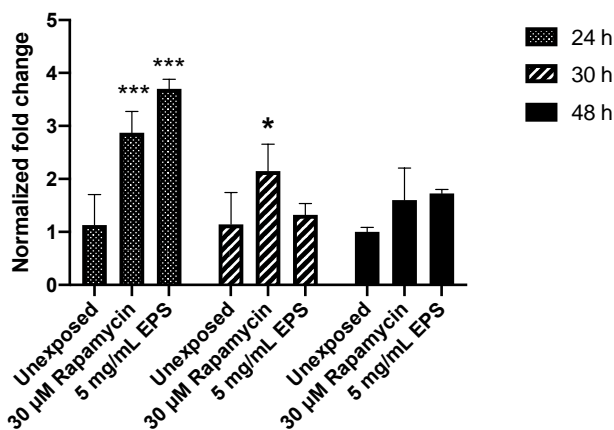


**Figure 15:** mRNA expression of GRP78 was upregulated in EPS from *B. pseudocatenulatum* ATCC 27919-exposed cells and Rapamycin-exposed cells at 24 h but reduced in an extended time compared to unexposed cells. Data were expressed as mean  $\pm$  SD. \* $p$ <0.05, \*\*\* $p$ <0.001 compared to the negative control (unexposed cells),  $n$ =3.

Rapamycin for 30 and 48 h. However, the protein expression has less potency for the mentioned time point.

**EPS from *Bifidobacterium pseudocatenulatum* ATCC 27919 promoted upstream activation of the autophagy**

In the present study, we found that EPS exposure to Caco-2 cells facilitated the phosphorylation of AMPK. It was observed significantly at 30 and 48 h of EPS

exposure (Figure 14A). On the other hand, EPS exposure to the cells alleviated the phosphorylation of mTOR in the cells at all time points. The finding agreed with cells exposed to Rapamycin, the commercially available mTOR inhibitor (Figure 14 B).

**EPS from *Bifidobacterium pseudocatenulatum* ATCC 27919 enhanced mRNA expression of GRP78, marking an early indication of ER stress**

The mRNA expression of GRP78 was significantly upregulated at 24 h by  $3.7 \pm 0.17$ -fold compared to unexposed cells ( $p$ <0.001). In Rapamycin-exposed cells, the mRNA expression was also significantly increased by  $2.87 \pm 0.4$ -fold compared to the unexposed cells at 24 h ( $p$ <0.001). However, the mRNA expression was downregulated as the time extended to 30 and 48 h in EPS- and Rapamycin-exposed Caco-2 cells (Figure 15).

**DISCUSSION**

Probiotics derived-EPS including from *Bifidobacteria* has been regarded as safe (GRAS) and can be used for biological activities both *in vitro* and *in vivo* experimental (Angelin and Kavitha, 2020). Khalil *et al.* (2022) reported that EPS derived from a wide range of probiotics can induce cell death in CRC cells. In the present study, we investigated the potential anti-cancer of EPS from *B. pseudocatenulatum* ATCC 27919 on CRC and elucidated the underlying mechanisms. The findings demonstrated that EPS has induced cell death and associated apoptosis and autophagy in CRC cells by regulating the AMPK/mTOR signalling pathway. More interestingly, endoplasmic reticulum (ER) involvement in EPS-induced cell death in Caco-2 cells was also detected.

In the study, Rapamycin was used to induce autophagy in the Caco-2 cells (Galluzzi *et al.*, 2011) and it was proposed as a positive control group for the experiments. The findings indicated that rapamycin exposure was cytotoxic to the Caco-2 cells (Figure 2). Research has established a reduction in more than 50% of cell viability *in vitro* in different cell types, including neuroblastoma and HeLa cell lines with rapamycin exposure. Previous studies have proven that with autophagy induction, there was an increase in cell death in response to rapamycin treatment (Lin *et al.*, 2018; Rezaadeh *et al.*, 2020).

One of the significant anti-cancer aspects is the ability of a compound to induce cancer cell death. Our results demonstrated that the EPS reduced the cell viability in Caco-2 cells at 48-h exposure (Figure 1), suggesting that EPS is cytotoxic towards the cells and causes cell death. EPS exposure to the cells also affected the cells morphologically (Figure 3). The cells appeared shrunken, rounded and condensed with blebbing membrane and loss of contact with neighbouring cells prominently at 48 h, which are distinct morphological characteristics of apoptosis (George *et al.*, 2015; Suganya *et al.*, 2019). Apoptosis is an extensively studied programmed cell death modality in cancer. It is also featured by chromatin condensation and nuclear fragmentation. The study showed that most EPS-exposed Caco-2 cells were detached from the culture slide at 48 h. The remaining cells on the culture slide were presented with loss of shape, chromatin condensation (red arrow), nuclear fragmentation (yellow arrow) and formation of apoptotic bodies (Figure 4 and 5). Summarily, the findings matched the main features of apoptosis (Fink and Cookson, 2005) and were comparable to rapamycin-exposed cells. It can be deduced that EPS exposure has induced apoptosis in Caco-2 cells.

We further provide evidence to support the role of apoptosis in EPS-induced cell death in the Caco-2 cells. From the Annexin V and cell dead assay, upon EPS exposure, most of the cell populations shifted significantly to the early apoptosis quadrant (Figure 6C). It is inferred that EPS exposure induced apoptosis in the Caco-2 cells. It is also consistent with the findings on the morphological observation using DAPI staining. The image of EPS-exposed cells at 48 h in Figure 5E and 5F showed more chromatin condensation. According to Saraste and Pulkki (2000), the onset of apoptosis is distinguished morphologically by cell shrinkage and nuclear chromatin condensation. It is subsequently commemorated by nuclear condensation and fragmentation in the later stage (Saraste and Pulkki, 2000).

Exposure to EPS also arrested cells at the G2/M phase of the cell cycle and likewise was observed in rapamycin-exposed cells at 48 h (Figure 7). Cell cycle phases control cells' progress in response to DNA damage or halt them in the G2/M phase to allow for DNA repair. The findings suggested that intracellular DNA damage is challenging to repair. Hence, cell cycle arrest in the presence of severe DNA damage can result in apoptotic cell death (Stark and Taylor, 2004). In response

to DNA damage, cells activate PARP-1 to enhance accessibility for DNA restoration (Sousa *et al.*, 2012). Significant upregulation of mRNA PARP-1 expression was observed initially at 24 h, prompting the hypothesis of PARP-1 action towards DNA damage upon detection. As previously mentioned, EPS exposure at 48 h has arrested the cell cycle at the G2/M phase, implying the excessive and irreparable DNA damage and cells proceeded to cell death by apoptosis hence the downregulated mRNA expression at 30 and 48 h (Figure 10). Exposure to EPS also induced apoptosis in cells via increasing expression of cleaved caspase-3 protein over the time tested compared to unexposed cells (Figure 8). Increased protein expression in cleaved Caspase-3 was also observed in Rapamycin-exposed cells. However, there is a substantial difference between the expression from the EPS-exposed cells and Rapamycin-exposed cells, as Rapamycin caused highly expressed cleaved caspase-3 protein (Zhang *et al.*, 2007). The involvement of two counteracting pro- and anti-apoptotic Bcl-2 family members during the EPS exposure was studied, i.e., the expression of BAX and Bcl-2 genes (Figures 9 and 12B). As the exposure time extended to 48 h, the mRNA expression of BAX increased significantly in unexposed cells. The result was lined with cells exposed to Rapamycin at 48 h.

Nonetheless, EPS exposure to the cells significantly downregulated the expression of the anti-apoptotic gene, Bcl-2, regardless of the time exposed. It was followed by similar observation in Rapamycin-exposed cells. The present study showed that EPS enhanced pro-apoptotic mRNA BAX expression while downregulating anti-apoptotic mRNA Bcl-2 expression in Caco-2 cells, increasing the BAX/Bcl-2 ratio. Our findings parallel with Zhu *et al.* (2015), as apoptosis was reported in human adipocytes exposed to Curcumin. It resulted from increased mRNA BAX expression and decreased mRNA Bcl-2 expression, hence the elevation of the BAX/Bcl-2 ratio (Zhu *et al.*, 2015).

Our data also suggest the role of autophagy in EPS-induced Caco-2 cells. The evidence includes increased LC3-II protein expression significantly at 24 h of EPS exposure compared to unexposed cells (Figure 11). LC3-II turnover indicates autophagic activity (Devenport and Shah, 2019). Accumulating evidence has proven that LC3-II is part of the autophagy process as its expression decreases when cells are exposed to the autophagy inhibitor, 3-Methyladenine (MA) (Zhu *et al.*, 2020; Yang *et al.*, 2021). A study was reported on restored autophagy by EPS from *B. animalis*, where LC3-II was observed to be enhanced in the intestinal porcine epithelial cell line (IPEC-J2) (Yuan *et al.*, 2021).

EPS exposure in Caco-2 cells upregulated the protein expression of p62 at 24 h before decreasing as the time extended to 48 h (Figure 13). Despite the substrate sequestering role in the phagosome, p62 is a linking adapter between LC3 and ubiquitinated substrates and is finally degraded by autophagy (Johansen and Lamark, 2011). The initial increase in the protein expression is correlated with the rise of LC3-II at 24 h. It is supported by

a study whereby p62 was notably increased consistently with LC3B-II after 1-4 h of amino acid starvation (Cohen-Kaplan *et al.*, 2016). In the present study, the subsequent downregulated expression of p62 preliminarily reflected the degradation of p62, suggesting the autophagic flux has been activated. Inhibition of autophagy is associated with elevated levels of p62 in mammals and *Drosophila*, implying that stable state levels of this protein reflect the autophagic status. On the contrary, decreased p62 levels are associated with autophagy activation (Klionsky *et al.*, 2016).

On the onset of autophagy, Beclin-1 is essential in initiating autophagosome. In the present study, the mRNA expression of Beclin-1 was significantly upregulated in EPS-exposed Caco-2 cells at 24 h (Figure 12A). It is consistent with a study that demonstrated the induction of autophagy activity with the appearance of autophagic vacuoles and highly expressed autophagy markers LC3-II and Beclin-1 in Evodiamine exposed to SW480 colon cancer cells (Wang *et al.*, 2019). According to Liu *et al.* (2017), the inhibition of Beclin-1 by RNA silencing has suppressed the autophagic activity in the colorectal cancer cells, HCT116 and SW620, which has caused decreased cell viability and increased apoptosis rate (Liu *et al.*, 2017). It explains the downregulation of Beclin-1 mRNA expression during the extended EPS exposure time of 48 h.

Beclin-1 binds to Bcl-2, the apoptosis-inhibiting factor. Classically, Bcl-2 is said to maintain autophagy levels at the physiological range (Pattingre *et al.*, 2005). In addition to the critical cytoprotective role of antagonizing BAX, Bcl-2 is an autophagy initiator by exerting inhibitory effects on autophagy via interaction with Beclin-1 (Xu and Qin, 2019). Our data support this notion by demonstrating downregulated mRNA expression of Bcl-2 (Figure 12B) at 24 h. In contrast, the high expression of Beclin-1 mRNA (Figure 12A) and highly expressed LC3-II protein (Figure 11) suggests the autophagy event.

AMPK/mTOR signaling is one of the classical autophagy regulatory pathways. AMPK is the upstream regulatory molecule of mTOR that negatively modulates the pathway. While mTOR responds to cellular environmental and nutrient level changes, AMPK is a cellular energy receptor activated when low ATP levels occur. mTOR and AMPK cooperatively activate ULK1 to cope with the changes, initiating autophagy (Hu *et al.*, 2021). In the present study, we found that EPS exposure increased the phosphorylation of AMPK while reducing the phosphorylation of mTOR (Figure 14A and 14B). Upregulation of mTOR signalling enhances tumour growth and development via suppression of autophagy (Saxton and Sabatini, 2017). A previous study reported similar findings in which a new anti-tumour drug, B-elemene, inhibits cell proliferation by inducing autophagy and apoptosis mechanism in human CRC cells. In the experiment, they observed a significant reduction of phosphorylated mTOR, suggesting that the mTOR pathway is one of the contributing effects (Wang *et al.*, 2022). The findings agreed with our data, suggesting that

EPS can negatively affect mTOR activity, enhancing autophagy.

On the other hand, the critical role of AMPK in autophagy regulation is illustrated with the knockdown of AMPK by shRNA on HCT116 and HT29 colon cancer cells exposed to a natural compound, Fangchinoline. It demonstrated a decrease in LC3-II / I ratio and autophagic flux, indicating no progress in the autophagy mechanism. Hence, it is suggested that AMPK plays an essential role in regulating autophagy (Xiang *et al.*, 2021).

Apoptosis and autophagy are both affected by various molecules, implying the switching between these biological processes in response to signaling from cell damage. Currently, relevant studies have indicated that nodes of interaction such as Bcl-2 and Beclin-1 interaction, p62, caspases and p53 are essential in controlling the interactions between autophagy and cell death in various cancers, including colorectal cancer (Qian *et al.*, 2017; Xie *et al.*, 2020). However, a molecule like GRP78, which is an uncommon molecule, may associate apoptosis and autophagy.

GRP78 is one of the ER stress sensors. ER stress is caused by the accumulation of deformed proteins that affect the ability of ER to fold proteins. In response to that, unfolded protein response (UPR) is activated upon dissociation of GRP78 from ER transmembrane receptor proteins (PERK, IRE1a and ATF6) (Deegan *et al.*, 2013; Chipurupalli *et al.*, 2021). The degradation of these aberrant proteins is mediated by ER-associated degradation (ERAD) by proteasome. However, continuous ER stress may lead to autophagy and is promoted by the elevation of GRP78 (La *et al.*, 2017). It is evidenced in the present study markers related to the onset of autophagy were increased at 24 h, such as LC3-II and Beclin-1, correlated to the upregulated GRP78 mRNA expression in Caco-2 cells exposed to EPS (Figure 15). A similar discovery was observed when HCT-116 and DLD1 triggered ER stress-induced autophagy, and berberine increased GRP78 expression in colon cancer cells. On the other hand, the effect of berberine on cell autophagy was attenuated when GRP78 was knocked down (La *et al.*, 2017). The idea is that ER stress-induced autophagy is a cytoprotective reaction to ensure the survival of cells. However, prolonged ER stress activates the caspase-mediated apoptosis pathway (Szegezdi *et al.*, 2006). In the current work, GRP78 mRNA expression in Caco-2 cells exposed to EPS was reduced after 48 h of exposure. As shown by concurrently decreased Bcl-2 mRNA expression, increased BAX mRNA expression, and increased levels of cleaved caspase-3 protein, GRP78 mRNA expression elevation resulted in a potent induction of apoptosis, which was consistent with the findings of the current study (Ou *et al.*, 2014).

In EPS exposure to Caco-2 cells, autophagy has preceded apoptosis. The cells exposed to EPS markedly boosted the expression of LC3-II protein, an essential autophagy marker, in contrast to unexposed cells at 24 h before it decreased in a time-dependent manner at 30 and 48 h. Additionally, it was discovered that Beclin-1

mRNA expression was much higher in EPS-exposed cells than in control cells after 24 h, which is a crucial step in the induction of autophagy. As time passed to 48 h, the mRNA expression continued to decline. It suggested the occurrence of autophagy event at 24 h. On the other hand, cleaved caspase-3 was observed in a time-dependent (24 to 48 h), and the increase is significant when compared to unexposed Caco-2 cells. These results were in accordance with a study by Yang *et al.* (2021). The amount of cleaved caspase-3, a downstream caspase effector, also increased, indicating that apoptosis was initiated in the later event. One intriguing theory is that decreased AMPK activation creates extreme energy depletion, which causes autophagy to decelerate. Hence, the cells went through apoptosis due to ineffective autophagy (Rodríguez-Vargas *et al.*, 2012; Dziaman *et al.*, 2014; Tempka, 2018).

## CONCLUSION

Research findings suggest the specific anti-cancer effect of EPS from *B. pseudocatenuatum* ATCC 27919 in Caco-2 cells. Exposure of Caco-2 cells to EPS suppressed cell viability by activating caspase-dependent apoptosis. Before apoptosis, there was EPS-induced autophagy, which plays a crucial part in cell death in ER stress. It was also indicated that the potential anti-cancer effect of EPS on colorectal cancer was achieved by upstream activation of the AMPK/mTOR pathway. Future research on the interaction between apoptosis and autophagy in EPS exposure may reveal novel therapeutic targets for treating colorectal cancer.

## ACKNOWLEDGEMENTS

This author gratefully acknowledges the financial support from the Ministry of Higher Education (KPT) Malaysia via the Fundamental Research Grant Scheme (FRGS) (Grant no. FRGS/1/2017/WAB11/UiTM/02/2). In addition, this work was also supported by Research Management Center (RMC), Universiti Teknologi MARA (UiTM), Malaysia.

## CONFLICT OF INTEREST

The authors declare that there is no conflict of interest regarding the publication of this manuscript.

## REFERENCES

- Angelin, J. and Kavitha, M. (2020). Exopolysaccharides from probiotic bacteria and their health potential. *International Journal of Biological Macromolecules* **162**, 853-865.
- Anukam, K. C. and Reid, G. (2007). Probiotics: 100 years (1907-2007) after Elie Metchnikoff's observation. *Communicating Current Research and Educational Topics and Trends in Applied Microbiology* **2**, 466-474.
- Azizah, A. M., Hashimah, B., Nirmal, K., Siti Zubaidah, A. R., Puteri, N. A., Nabihah, A. *et al.* (2019). Malaysia National Cancer Registry Report (MNCR) 2012-2016. National Cancer Registry, Malaysia.
- Bata, N. and Cosford, N. D. P. (2021). Cell survival and cell death at the intersection of autophagy and apoptosis: Implications for current and future cancer therapeutics. *ACS Pharmacology and Translational Science* **4(6)**, 1728-1746.
- Bhardwaj, M., Leli, N. M., Koumenis, C. and Amaravadi, R. K. (2020). Regulation of autophagy by canonical and non-canonical ER stress responses. *Seminars in Cancer Biology* **66**, 116-128.
- Chipurupalli, S., Samavedam, U. and Robinson, N. (2021). Crosstalk between ER stress, autophagy and inflammation. *Frontiers in Medicine* **8**, 758311.
- Cohen-Kaplan, V., Livneh, I., Avni, N., Fabre, B., Ziv, T., Kwon, Y. T. *et al.* (2016). p62- and ubiquitin-dependent stress-induced autophagy of the mammalian 26S proteasome. *Proceedings of the National Academy of Sciences of the United States of America* **113(47)**, E7490-E7499.
- Deegan, S., Saveljeva, S., Gorman, A. M. and Samali, A. (2013). Stress-induced self-cannibalism: On the regulation of autophagy by endoplasmic reticulum stress. *Cellular and Molecular Life Sciences* **70(14)**, 2425-2441.
- Devenport, S. N. and Shah, Y. M. (2019). Functions and implications of autophagy in colon cancer. *Cells* **8(11)**, 1349.
- Dossou, A. S. and Basu, A. (2019). The emerging roles of mTORC1 in macromanaging autophagy. *Cancers* **11(10)**, 1422.
- Duar, R. M., Lin, X. B., Zheng, J., Martino, M. E., Grenier, T., Pérez-Muñoz, M. E. *et al.* (2017). Lifestyles in transition: Evolution and natural history of the genus *Lactobacillus*. *FEMS Microbiology Reviews* **41**, 27-48.
- Dziaman, T., Ludwiczak, H., Ciesla, J. M., Banaszkiwicz, Z., Winczura, A., Chmielarczyk, M. *et al.* (2014). PARP-1 expression is increased in colon adenoma and carcinoma and correlates with OGG1. *PLoS ONE* **9(12)**, e115558.
- El-Deeb, N. M., Yassin, A. M., Al-Madboly, L. A. and El-Hawiet, A. (2018). A novel purified *Lactobacillus acidophilus* molecularly regulates both apoptotic and NF- $\kappa$ B inflammatory pathways in human colon cancer. *Microbial Cell Factories* **17**, 29.
- FAO/WHO, Food and Agriculture Organization of the United Nations/ World Health Organization. (2006). Probiotics in food: Health and nutritional properties and guidelines for evaluation. World Health Organization/Food and Agriculture Organization of the United Nations, Rome.
- Fink, S. L. and Cookson, B. T. (2005). Apoptosis, pyroptosis and necrosis: Mechanistic description of dead and dying eukaryotic cells. *Infection and Immunity* **73(4)**, 1907-1916.
- Galluzzi, L., Morselli, E., Kepp, O., Vitale, I., Younes, A. B., Maiuri, M. C. *et al.* (2011). Evaluation of

- rapamycin-induced cell death, *In: mTOR. Methods in Molecular Biology*. Weichhart, T. (eds.). Humana Press, Totowa, NJ. pp 125-169.
- George, B. P. A., Tynga, I. M. and Abrahamse, H. (2015).** *In vitro* anti-proliferative effect of the acetone extract of *Rubus fairholmianus* Gard. root on human colorectal cancer cells. *BioMed Research International Article ID 165037*.
- Hu, C., Cao, Y., Li, P., Tang, X., Yang, M., Gu, S. et al. (2021).** Oleanolic acid induces autophagy and apoptosis via the AMPK-mTOR signaling pathway in colon cancer. *Journal of Oncology Article ID 8281718*.
- International Agency for Research on Cancer. (2020).** Colorectal cancer. Number of new cases in 2020. Globocan 2020, World Health Organization.
- Jangamreddy, J. R., Pantgrahi, S. and Los, M. J. (2015).** Monitoring of autophagy is complicated-salinomycin as an example. *Biochimica et Biophysica Acta (BBA) - Molecular Cell Research 1853(3)*, 604-610.
- Jeong, J. J., Park, H. J., Cha, M. G., Park, E., Won, S. M., Ganesan, R. et al. (2022).** The *Lactobacillus* as a probiotic: Focusing on liver diseases. *Microorganisms 10(2)*, 288.
- Johansen, T. and Lamark, T. (2011).** Selective autophagy is mediated by autophagic adapter proteins. *Autophagy 7(3)*, 279-296.
- Khalil, M. A., Sonbol, F. I., Al-Madboly, L. A., Aboshady, T. A., Alqurashi, A. S. and Ali, S. S. (2022).** Exploring the therapeutic potentials of exopolysaccharides derived from lactic acid bacteria and bifidobacteria: Antioxidant, antitumor, and periodontal regeneration. *Frontiers in Microbiology 13*, 803688.
- Klionsky, D. J., Abdelmohsen, K., Abe, A., Abedin, M. J., Abeliovich, H., Arozana, A. A. et al. (2016).** Guidelines for the use and interpretation of assays for monitoring autophagy Edn. 3<sup>rd</sup>. *Autophagy 12(1)*, 1-222.
- La, X., Zhang, L., Li, Z., Yang, P. and Wang, Y. (2017).** Berberine-induced autophagic cell death by elevating GRP78 levels in cancer cells. *Oncotarget 8(13)*, 20909-20924.
- Li, X., He, S. and Ma, B. (2020).** Autophagy and autophagy-related proteins in cancer. *Molecular Cancer 19(1)*, 12.
- Lin, X., Han, L., Weng, J., Wang, K. and Chen, T. (2018).** Rapamycin inhibits proliferation and induces autophagy in human neuroblastoma cells. *Bioscience Reports 38(6)*, BSR20181822.
- Liu, L., Zhao, W. M., Yang, X. H., Sun, Z. Q., Jin, H. Z., Lei, C. et al. (2017).** Effect of inhibiting Beclin-1 expression on autophagy, proliferation and apoptosis in colorectal cancer. *Oncology Letters 14(4)*, 4319-4324.
- Lu, Y., Wang, J., Ji, Y. and Chen, K. (2019).** Metabonomic variation of exopolysaccharide from *Rhizopus nigricans* on AOM/DSS-induced colorectal cancer in mice. *OncoTargets and Therapy 12*, 10023-10033.
- Ministry of Health Malaysia. (2021).** National Strategic Plan for Colorectal Cancer (NSPCRC) 2021-2025. Ministry of Health Malaysia, Putrajaya, Malaysia.
- Oerlemans, M. M. P., Akkerman, R., Ferrari, M., Walvoort, M. T. C. and de Vos, P. (2021).** Benefits of bacteria-derived exopolysaccharides on gastrointestinal microbiota, immunity and health. *Journal of Functional Foods 76*, 104289.
- Ou, Y., Xu, S., Zhu, D. and Yang, X. (2014).** Molecular mechanisms of exopolysaccharide from *Aphanothece halaphytica* (EPSAH) induced apoptosis in HeLa cells. *PLoS ONE 9(1)*, e87223.
- Pattingre, S., Tassa, A., Qu, X., Garuti, R., Xiao, H. L., Mizushima, N. et al. (2005).** Bcl-2 antiapoptotic proteins inhibit Beclin 1-dependent autophagy. *Cell 122(6)*, 927-939.
- Qian, H. R., Shi, Z. Q., Zhu, H. P., Gu, L. H., Wang, X. F. and Yang, Y. (2017).** Interplay between apoptosis and autophagy in colorectal cancer. *Oncotarget 8(37)*, 62759-62768.
- Rah, B., Rasool, R., Nayak, D., Yousuf, S. K., Mukherjee, D., Kumar, L. D. et al. (2015).** PAWR-mediated suppression of BCL2 promotes switching of 3-azido withaferin A (3-AWA)-induced autophagy to apoptosis in prostate cancer cells. *Autophagy 11(2)*, 314-331.
- Rezazadeh, D., Norooznezhad, A. H., Mansouri, K., Jahani, M., Mostafaie, A., Mohammadi, M. H. et al. (2020).** Rapamycin reduces cervical cancer cells viability in hypoxic condition: Investigation of the role of autophagy and apoptosis. *OncoTargets and Therapy 13*, 4239-4247.
- Rodríguez-Vargas, J. M., Ruiz-Magãa, M. J., Ruiz-Ruiz, C., Majuelos-Melguizo, J., Peralta-Leal, A., Rodríguez, M. I. et al. (2012).** ROS-induced DNA damage and PARP-1 are required for optimal induction of starvation-induced autophagy. *Cell Research 22(7)*, 1181-1198.
- Saraste, A. and Pulkki, K. (2000).** Morphologic and biochemical hallmarks of apoptosis. *Cardiovascular Research 45(3)*, 528-537.
- Saxton, R. A. and Sabatini, D. M. (2017).** mTOR signaling in growth, metabolism and disease. *Cell 168(6)*, 960-976.
- Sousa, F. G., Matuo, R., Soares, D. G., Escargueil, A. E., Henriques, J. A. P., Larsen, A. K. et al. (2012).** PARPs and the DNA damage response. *Carcinogenesis 33(8)*, 1433-1440.
- Stark, G. R. and Taylor, W. R. (2004).** Analyzing the G2/M checkpoint. *In: Methods in Molecular Biology™: Checkpoint Controls and Cancer*. Schönthal, A.H. (eds). Humana Press, Totowa, New Jersey. pp. 51-82.
- Suganya, M., Gnanamangai, B. M., Ravindran, B., Chang, S. W., Selvaraj, A., Govindasamy, C. et al. (2019).** Antitumor effect of proanthocyanidin induced apoptosis in human colorectal cancer (HT-29) cells

- and its molecular docking studies. *BMC Chemistry* **13(3)**, 21.
- Sungur, T., Aslim, B., Karaaslan, C. and Aktas, B. (2017).** Impact of exopolysaccharides (EPSs) of *Lactobacillus gasseri* strains isolated from human vagina on cervical tumor cells (HeLa). *Anaerobe* **47**, 137-144.
- Szegezdi, E., Logue, S. E., Gorman, A. M. and Samali, A. (2006).** Mediators of endoplasmic reticulum stress-induced apoptosis. *EMBO Reports* **7(9)**, 880-885.
- Tempka, D., Tokarz, P., Chmielewska, K., Kluska, M., Pietrzak, J., Rygielska, Z. et al. (2018).** Downregulation of PARP1 transcription by CDK4/6 inhibitors sensitizes human lung cancer cells to anti-cancer drug-induced death by impairing OGG1-dependent base excision repair. *Redox Biology* **15**, 316-326.
- Wang, D., Ge, S., Chen, Z. and Song, Y. (2019).** Evodiamine exerts anti-cancer effects via induction of apoptosis and autophagy and suppresses the migration and invasion of human colon cancer cells. *Journal of B.U.ON.* **24(5)**, 1824-1829.
- Wang, G. Y., Zhang, L., Geng, Y. Di., Wang, B., Feng, X. J., Chen, Z. L. et al. (2022).**  $\beta$ -Elemene induces apoptosis and autophagy in colorectal cancer cells through regulating the ROS/AMPK/mTOR pathway. *Chinese Journal of Natural Medicines* **20(1)**, 9-21.
- Wu, J., Zhang, Y., Ye, L. and Wang, C. (2021).** The anti-cancer effects and mechanisms of lactic acid bacteria exopolysaccharides *in vitro*: A review. *Carbohydrate Polymers* **253**, 117308.
- Xi, H., Wang, S., Wang, B., Hong, X., Liu, X., Li, M. et al. (2022).** The role of interaction between autophagy and apoptosis in tumorigenesis (Review). *Oncology Reports* **48(6)**, 208.
- Xiang, X., Tian, Y., Hu, J., Xiong, R., Bautista, M., Deng, L. et al. (2021).** Fangchinoline exerts anti-cancer effects on colorectal cancer by inducing autophagy via regulation AMPK/mTOR/ULK1 pathway. *Biochemical Pharmacology* **186**, 114475.
- Xie, Q., Liu, Y. and Li, X. (2020).** The interaction mechanism between autophagy and apoptosis in colon cancer. *Translational Oncology* **13(12)**, 100871.
- Xu, H. D. and Qin, Z. H. (2019).** Beclin 1, Bcl-2 and autophagy. *In: Autophagy: Biology and Diseases. Advances in Experimental Medicine and Biology.* Qin, Z. H. (eds.). Springer, Singapore. pp. 109-126.
- Yang, H. L., Liu, H. W., Shrestha, S., Thiyagarajan, V., Huang, H. C. and Hseu, Y. C. (2021).** *Antrrodia salmonea* induces apoptosis and enhances cytoprotective autophagy in colon cancer cells. *Aging* **13(12)**, 15964-15989.
- Yaziz, H. N. M., Zulkipli, H., Adenan, M. I., Musa, M., Kasmuri, N. and Khalil, K. A. (2021).** Statistical optimization of cultivation parameters for exopolysaccharides production by *Bifidobacterium pseudocatenulatum* ATCC 27919 in glutinous rice water medium. *Malaysian Journal of Biochemistry and Molecular Biology* **24(3)**, 69-76.
- Yuan, L., Chu, B., Chen, S., Li, Y., Liu, N., Zhu, Y. et al. (2021).** Exopolysaccharides from *Bifidobacterium animalis* ameliorate *Escherichia coli*-induced IPEC-J2 cell damage via inhibiting apoptosis and restoring autophagy. *Microorganisms* **9(11)**, 2363.
- Zahran, W. E., Elsonbaty, S. M. and Moawed, F. S. M. (2017).** *Lactobacillus rhamnosus* ATCC 7469 exopolysaccharides synergizes with low level ionizing radiation to modulate signaling molecular targets in colorectal carcinogenesis in rats. *Biomedicine and Pharmacotherapy* **92**, 384-393.
- Zhang, J. F., Liu, J. J., Lu, M. Q., Cai, C. J., Yang, Y., Li, H. et al. (2007).** Rapamycin inhibits cell growth by induction of apoptosis on hepatocellular carcinoma cells *in vitro*. *Transplant Immunology* **17(3)**, 162-168.
- Zhu, L., Han, M. B., Gao, Y., Wang, H., Dai, L., Wen, Y. et al. (2015).** Curcumin triggers apoptosis via upregulation of Bax/Bcl-2 ratio and caspase activation in SW872 human adipocytes. *Molecular Medicine Reports* **12(1)**, 1151-1156.
- Zhu, M. L., Zhang, P. M., Jiang, M., Yu, S. W. and Wang, L. (2020).** Myricetin induces apoptosis and autophagy by inhibiting PI3K/Akt/mTOR signalling in human colon cancer cells. *BMC Complementary Medicine and Therapies* **20(1)**, 209.